GEOLOGICAL SURVEY OF CANADA

OPEN FILE 4934

Gas hydrate concentration estimates from chlorinity, electrical resistivity and seismic velocity

M. Riedel, T.S. Collett, R.D. Hyndman

2005

Natural Resources
Canada

Ressources naturelles
Canada

Canada

GEOLOGICAL SURVEY OF CANADA

OPEN FILE 4934

Gas hydrate concentration estimates from chlorinity, electrical resistivity and seismic velocity

M. Riedel, T.S. Collett, and R.D. Hyndman

2005

Open files are products that have not gone through the GSC formal publication process.

Gas hydrate concentration estimates from chlorinity, electrical resistivity and seismic velocity

M. Riedel[1], T.S. Collett[2], and R.D. Hyndman[1]

(1) Natural Resources Canada, Geological Survey of Canada, Pacific Geoscience Centre, 9860 West Saanich Road, Sidney, British Columbia, V8L 4B2

(2) US Geological Survey, Denver Federal Center, PO Box 25046, MS-939 Denver, Colorado, 80225

ABSTRACT

Gas hydrate beneath the N. Cascadia continental slope off Vancouver Island occurs as a regional diffuse layer above the BSR and as local high concentrations in large vent or upwelling structures. Regional concentrations of gas hydrate beneath the N. Cascadia continental slope off Vancouver Island have been estimated earlier using multichannel seismic, seafloor electrical, and IODP Leg 146 downhole data. The concentrations of between 15 and 30% of pore saturation in a 100 m thick layer above the BSR are much higher than estimated elsewhere where there is good data, especially the Blake Ridge and central Cascadia off Oregon on ODP Leg 204. Although both of these other studies involved different sediment environments, a careful re-evaluation of the N. Cascadia estimates seemed desirable. We have re-evaluated the methods used to calculate the gas hydrate concentrations from pore-water chlorinity (salinity), electrical resistivity, and seismic velocity, describing in detail the assumptions and uncertainties. Use of the pore-water chlorinity/salinity and electrical resistivity directly have low reliability because of the effect on the no-hydrate reference of hydrate formation and dissociation, and the effect of pore fluid freshening by clay dehydration. At ODP Site 889/890 hydrate concentrations range from 5–10% to 30–40%, depending on the no-hydrate reference salinity used. Use of core salinity data along with the downhole and seafloor electrical resistivity data allows calculation of both the in situ reference salinity and the hydrate concentrations. The most important uncertainty in this method is the relation between

resistivity and porosity, i.e., Archie's Law parameters. Significantly different relations were determined from the ODP Leg 146 core and downhole log data, the log data resistivity-porosity relation giving much lower concentrations. Finally, seismic velocities from sonic-logs and multichannel data can be used to calculate gas hydrate concentrations, if an appropriate no-hydrate velocity-depth profile can be estimated. A velocity-hydrate concentration relation is also required. Depending on which no-hydrate/no-gas velocity baseline is used, estimated hydrate concentrations range from as low as 5% to above 25% saturation. In spite of having three nearly independent methods of estimating hydrate concentrations, it is concluded that the data allow regional concentrations in the 100 m layer above the BSR from less than 5% to over 25% saturation (3-13% of sediment volume). ODP drilling in the region scheduled for the fall of 2005 should help resolve the uncertainties.

INTRODUCTION

The presence of gas hydrate has been established on Canada's West Coast at the Northern Cascadia Margin by widespread bottom simulating reflectors (BSR) in multichannel seismic (MCS) data, by scientific drilling by the Ocean Drilling Program (ODP) Leg 146, and by electrical sounding (for summaries of those studies see Hyndman et al., 2001; Spence et al., 2000 and references therein). The BSR was observed in a 20-30 km wide band along much of the 250 km length of the Vancouver Island continental slope (**Figure 1**). After the first discovery of BSRs in 1985, the area offshore Vancouver Island has been the focus of many interdisciplinary studies. Studies include 2D and 3D single channel and multichannel conventional and high-resolution seismic studies (Yuan et al., 1996, 1999; Fink and Spence, 1999; Riedel et al., 2002; Chapman et al., 2002; Gettrust et al., 1999), vertical seismic profiling (MacKay et al., 1994), Ocean Bottom Seismometer (OBS) surveys (Spence et al, 1995; Hobro 1999), swath-bathymetry mapping, high-resolution subbottom profiling, heat-flow studies (Ganguly et al., 2000), piston coring with geochemical and geophysical sediment analyses (Novosel, 2002; Solem et al., 2002), ODP scientific drilling Leg 146 (Westbrook et al., 1994), seafloor electrical sounding (Edward, 1997; Yuan and Edwards, 2001), and ocean bottom video surveying with the remotely operated vehicle ROPOS (Riedel et al., 2002).

Gas hydrate concentrations were previously calculated from the ODP downhole sonic and resistivity logs, MCS interval and vertical seismic profile (VSP) velocities and from pore-water freshening (e.g. Yuan et al., 1996, 1999; Hyndman et al., 1999). Gas hydrate concentrations from the different methods differ slightly, but were estimated to be on average 20 – 35 % of the pore space over a 100 m thick interval above the BSR. One contrasting estimate was that by Ussler and Paull (2001) interpreting chlorinity data from ODP Leg 146 by using a smooth chlorinity baseline. They assumed that the general pore fluid freshening in recovered cores was mainly due to sources other than hydrate dissociation. This approach suggested much lower gas hydrate concentrations at Site 889/890.

These are unusually high gas hydrate concentrations for a marine gas hydrate occurrence, much higher than on the two other margins where there is sufficient data for quantitative estimates. ODP drilling and logging at the Blake Ridge offshore South Carolina (passive Margin environment) showed gas hydrate concentrations that were on average lower than 10% (Paull et al., 1996). ODP Leg 204 which was located at southern Hydrate Ridge on the southern Cascadia Margin offshore Oregon, has a similar tectonic environment to northern Cascadia. That area showed low gas hydrate concentrations of less than 5% except for the unusual summit of Hydrate Ridge (Trehu et al., 2004). It is this difference between northern Cascadia hydrate concentration estimates and those for Blake Ridge and Hydrate Ridge that prompted this re-evaluation of the northern Cascadia concentration estimates.

We note that both Blake Ridge and Hydrate Ridge have important differences in environment compared to northern Cascadia that could explain the differences in hydrate concentrations. Blake Ridge is on a passive rifted margin with the hydrate being mainly in deep sea contour drift deposits of fine grain sediments. The upward fluid motion that may carry methane upward into the hydrate stability field is quite low compared to estimates for Cascadia. In the ODP drilling at Hydrate Ridge, the upper sediment sections penetrated by the wells to the BSR were all in slope basin sediments, i.e., young sediments deposited on top of the older accretionary wedge sediments originally deposited on the deep sea floor. The limited time for hydrate formation since slope basin sediment deposition may limit the concentrations. Accreted sediments were penetrated,

but only below the BSRs. In contrast, at northern Cascadia Leg 146 Site 889/890, the sediments in the ~100 m above the BSR are accretionary prism sediments. This is the interval where the highest concentrations of hydrate have been inferred. These sediments are much older than the slope basin sediments so have had more time for hydrate formation.

In the following sections we review three different methods of calculating gas hydrate concentrations from: (a) pore-water freshening using chlorinity data, (b) electrical resistivity from logs and core data, and (c) from acoustic data (sonic logs and multichannel seismic interval velocities). The emphasis is on discussing the underlying assumptions and uncertainties in empirical parameters required for these methods and their effect on gas hydrate concentrations, rather than to present a new model for the northern Cascadia Margin. The work should provide an important background to the new IODP drilling planned for 2005. At present, the availability and quality of drilling, core and logging data do not allow a unique model, in contrast to, for instance, southern Hydrate Ridge where there is more recent and definitive data.

CHLORINITY AND PORE-WATER FRESHENING

Estimating in situ pore water chlorinity/salinity

When gas hydrate forms in marine sediments the process initially increases the salinity of the remaining pore-water because the salt in the saline pore fluid is not incorporated into the gas hydrate crystals. Assuming slow gas hydrate formation, it is expected that over long periods of time the excess salt will be removed by upward pore-fluid migration from beneath the hydrate stability field. The pore-water chlorinity/salinity will return to the equilibrium concentrations below the BSR, which is usually close to that of seawater. When a core sample is retrieved, any gas hydrate present *in situ* usually will have dissociated by the time a pore-water sample is analyzed. The dissociation of gas hydrate releases methane and fresh water, thus pore water that is fresher than the assumed background level is an indication of the presence of gas hydrate. This process has been used widely to estimate gas hydrate concentrations (e.g. Hesse and Harrison, 1981; Hesse, 2003; Kastner et al., 1995; Ussler and Paull, 2001). However, the limitation of the method is the problem of estimating the *in situ* pore fluid chlorinity/salinity. The

pore fluid chlorinity/salinity in deep sea sediments is commonly found to be approximately seawater. For example, near seawater pore water chlorinity/salinity was found for Leg 146 deep sea reference hole 888 in Cascadia Basin. However, in contrast to deep sea basin sediments, seawater pore water chlorinity/salinity may not be valid in accretionary prism sediments, the environment of Site 889/890 hydrate formation (e.g., Torres et al., 2004).

There are several processes (hydrate and non-hydrate related) that can result in in situ chlorinity/salinity that is higher or lower than seawater at the depths of hydrate occurrence: (a) the more saline pore fluid produced at the time of hydrate formation is not completely flushed upward and replaced with seawater salinity pore fluid, the chorinity/salinity may be higher than seawater, (b) fresh water from the dissociation of hydrate as the base of the stability field moves upward due to prism thickening. This low salinity pore water may be carried upward to shallow depths, (c) paleo-oceanographic seawater salinity changes, especially Pleistocene, (d) dehydration of clay (smectite) minerals at greater depth (T > 100ºC) and other non-hydrate related processes followed by upward migration of these fresher fluids by tectonic compression (e.g., Torres et al., 2004).

We note the general problem with salinity from pore water as measure for gas hydrate concentration is the relatively small sample density of typically one sample every 5 meter during ODP operations. Thus the retrieved profile is heavily spatially aliased and if thin layers are missed, gas hydrate concentrations may be underestimated. In a special experiment during Leg 204 (Torres et al., 2004, Trehu et al., 2003) pore-water measurements and infra-red (IR) scans of the core were compared and showed that if the pore-water sample was taken more than 10 cm away from a discrete gas hydrate occurrence, no chlorinity/salinity anomaly would be detected.

Estimating hydrate concentrations from core chlorinity at Site 889/890

The chlorinity versus depth profile at Site 889/890 (**Figure 2a**) is substantially fresher than seawater, ranging from near seawater just below the seafloor (530 mM) to about 35% fresher than seawater (360 mM) just above the BSR. This is an exceptionally low value for deep sea marine sediments. For example the ODP gas hydrate holes off

Oregon (Torres et al., 2005) and the MITI gas hydrate holes off SW Japan (Tomaru et al., 2004) showed much less freshening.

There is almost no discontinuity at the BSR. There is a small but hardly significant decrease in chlorinity with depth in the 100 m below the BSR. The lack of a discontinuity at the BSR may be interpreted as either, (a) there is little *in situ* hydrate; the general core pore fluid freshening is due to other geochemical processes, (b) there is substantial hydrate; the pore fluid below the BSR has been freshened by dissociation of hydrate formerly above the BSR, with the recent upward movement of the BSR due to accretionary prism tectonic uplift.

A slight decrease of pore-water salinity with depth was recognized at ODP reference Site 888 (**Figure 2b**) with a reduction of salinity from about PSU 35 (~560 mM chlorinity) at the seafloor to 32 PSU at 350 mbsf (~360 mM), that may be attributed to paleo-oceanographic seawater salinity changes. The use of the chlorinity/salinity profile at reference Site 888 as a baseline reference for Site 889 core data, gives substantial gas hydrate concentrations (e.g., Hyndman et al., 1999). The other model for the *in situ* pore-water salinity profile provides a minimum estimate of hydrate concentrations, i.e., using a smooth best-fit line through the measured data as the *in situ* reference (Ussler and Paull, 2001). Only small concentrations of hydrate are estimated using this reference.

It should be noted that the salinity profile at Site 889 (Figure 2b) shows a few distinct anomalies (especially between 100 and 150 mbsf) where salinity values are much higher than what the decreasing reference profile would suggest. Initially this was used as an argument for a seawater-like reference from Site 888 (Hyndman et al., 1999). However, the same samples that produced those suspicious high salinity values do not show an equivalent shift in chlorinity, questioning the reliability of these particular measurements.

It is clear that additional constraints are needed to reliably estimate the *in situ* pore fluid reference and thus the hydrate concentration from core chlorinity/salinity data.

Additional constraints come from, (a) geochemical data (such as lithium, Mg/Sr ratios and Sr isotopes) that indicate mixing of fluids (Torres et al., 2004; Kastner et al., 1995), and from integrating core salinity data with downhole electrical resistivity data.

We discuss the latter in a section below. Using geochemical data, Torres et al. (2004) postulated that the general downward freshening of pore water in recovered cores at Site 889/890 is not due to *in situ* hydrate, but rather due to other process such as dehydration of smectite clay to illite. Gas hydrate concentration is then independent of the general magnitude of the pore-water freshening with depth, and gas hydrate is only apparent as discrete low-Cl⁻ anomalies that overlay the general Cl⁻ trend. As part of their model, it is predicted that the *in situ* pore-water becomes progressively fresher landward with distance from the toe of the accretionary prism. In Leg 204 Sites 1244, 1251, and 125 off Oregon (12 to 19 km from deformation front), the chlorinity and salinity decrease gradually with depth (**Figure 2a**). This decrease was interpreted as the result of mixing of fresher pore fluids that were expelled from the deeper accretionary prism, i.e., in situ pore fluids that are freshened by up to 15% compared to seawater, due to geochemical processes. They suggested that Site 889/890 in northern Cascadia is in a more landward position in the accretionary wedge (22 km from deformation front) and should therefore have a further freshening of the pore water, in agreement with the ~35% freshening observed in the cores. Unfortunately, there is no strontium isotope data in cores from at Site 889/890 to substantial this model. Lacking measurements of strontium isotopes at this site, we simply assume (but still acknowledge that uncertainty) that the theory by Torres et al. (2004) is correct and that at Site 889 (22 km from the prism toe) a much more pronounced freshening from illitization has to occur than at southern Hydrate Ridge (12-19 km away from the toe).

ELECTRICAL RESISTIVITY

Gas hydrate concentrations may be estimated from downhole electrical resistivity (e.g., Collett, 2001) since, compared to the saline pore-water, gas hydrate is a nearly perfect insulator. Its presence can substantially increase the electrical resistivity of the sediments. The electrical resistivity log may be used directly if a no-hydrate reference resistivity versus depth is known. The electrical resistivity logs for Site 888 provide one type of reference for no-hydrate, no-gas. The resistivities at that site vary smoothly with depth, averaging about 1.0 ohm-m. This is a very common value for deep sea clastic

sediments. In the upper 100 m, the resistivity increases with depth due to sediment consolidation and porosity decrease with depth. At greater depth this factor becomes less important and the resistivity decreases with depth due to temperature increase. In contrast, the resistivity for Site 889/890 increases steadily to a value of about 2.1 ohm-m for the 100 m above the BSR and decreases somewhat below that depth. The difference between the basin and slope sites is unlikely due to differences in sediment type or porosity since; the slope site is concluded to have higher porosity, and lower expected porosity, at the same depths compared to the deep sea site (e.g., Yuan et al., 1994). If the in situ pore fluid salinity is similar at Site 889/890 to that at 888, the difference in resistivity provides an estimate of the hydrate concentration. However, as discussed above for salinity freshening estimates of hydrate concentrations, this may not be a valid assumption. The in situ pore fluid at hydrate Site 889/890 may be less saline and more resistive than at Cascadia Basin Site 888, and other approaches are needed to obtain an in situ pore fluid salinity as discussed below.

At the BSR there is no sharp resistivity discontinuity, but there is a significant downward decrease in resistivity to about 1.8 ohm-m at 30 m below the BSR. Assuming that there is substantial hydrate above the BSR, the lack of a discontinuity in resistivity may be explained by (a) a decrease in pore fluid salinity at that depth (assuming no sediment composition change) that has the opposite resistivity effect to the hydrate contrast. Such a salinity contrast is expected if the base of the hydrate stability field (BSR) is moving upward. Dissociating hydrate will leave behind low salinity pore fluid. (b) hydrate being formed around the borehole below the BSR by the drilling process. The free gas shown by the Vertical Seismic Profile (VSP) data to underlie the BSR may be converted to hydrate in an annulus around the hole. There is temperature reduction in the formation around the borehole from the cool drilling fluid which is at near seafloor temperature. Free gas itself should result in an increase in resistivity below the BSR rather than the observed decrease.

The resistivity-depth log may be used along with porosity-depth logs (neutron and density) or core porosities to estimate hydrate concentrations, if the *in situ* pore fluid resistivity (i.e., salinity) is known. To a first order, the porosities from the neutron and density logs will include the hydrate since it is expected to have a similar response to

pore fluid for these logs. In contrast, the porosities from the log resistivities (using Archie's law) exclude the hydrate, since the hydrate is electrically resistive. The differences between the two porosities provide estimates of hydrate concentrations. The critical unknown is the *in situ* pore fluid resistivity to be used in the Archie's law relation. The laboratory core pore fluid resistivity or salinity may be used, but these values are affected by the freshening due to dissociation of any hydrate that was present *in situ*. Fortunately, it is possible to estimate both the hydrate concentrations and the *in situ* salinities by integrating the downhole log resistivity data with core salinity and core porosity data, again using Archie's law (Hyndman et al., 1999). The Hyndman et al (1999) equation is again given in the appendix for completeness.

Resistivity-porosity relations; Archie's Law

All estimates of hydrate concentration using resistivity have assumed that formation of hydrate has nearly the same effect on resistivity as a reduction in porosity. This is a reasonable assumption but has not yet been well tested. The hydrate estimates are therefore dependent on the relation between sediment electrical resistivity (R_s), porosity (Φ), pore-water resistivity (R_f), and water saturation (S_w) as usually described by Archie's law:

$$R_s = a\, R_f\, \Phi^{-m}\, S_w^{-n} \qquad\qquad (2)$$

with the empirical Archie coefficients a, m, and n (e.g. Collett and Ladd, 2002). In case of purely water-saturated sediments (i.e. $S_w = 1.0$), Archie's law simplifies to

$$R_s = a\, R_f\, \Phi^{-m} \qquad\qquad (3)$$

Another simpler resistivity approach for assessing gas hydrate saturations ($S_h = 1 - S_w$) is the so-called "quick-look Archie" analysis technique, where the electrical resistivity of water-saturated sediment (R_0) is compared to the electrical resistivity of hydrate-bearing sediment (R_s):

$$S_w = (R_0\, /\, R_s)^{(1/n)} \qquad\qquad (4)$$

Parameters a and m

The most critical components in using electrical resistivity measurements to calculate gas hydrate concentrations are the empirical Archie coefficients a, m, and n. The parameters a and m in equation (2) are determined from purely water-saturated

sediments. Typically they are estimated from a log-log crossplot of formation factor (FF) as a function of porosity, generally known as "Pickett plot" (e.g. Serra, 1984). The slope of a best-fit linear trend through the data represents the parameter m, whereas parameter a is given by the intercept of such a best-fit line with the FF-axis at a porosity of $\Phi = 1$.

There are two sources of data to generate the FF-porosity crossplot, (a) data from discrete core samples, or (b) from downhole logging data. Each data type has important limitations. Core samples are available only at discrete intervals, and the core may be significantly altered from the *in situ* sediment conditions. A correction for temperature and pore-water salinity can be made. However, the sediment texture is often heavily altered, especially if larger amounts of gas hydrates were present *in situ*. Gas expansion cracks and so-called "moussy" or soupy textures develop and disrupt sediment fabric. Estimates of the parameter *a* and *m* from discrete core samples must therefore be taken with caution.

Downhole log data have important limitations; this is especially so for the neutron porosity and density log-based porosity data. Deep resistivity log data should be much more reliable. Log data are strongly degraded by poor bore-hole conditions, especially by enlargements by washouts. ODP boreholes are commonly enlarged because of the lack of drilling mud to provide hole wall stability. Logging-While-Drilling (LWD) data are generally preferable to wire-line (WL) log data because LWD data are less subject to hole enlargement. Also WL data are measured a considerable time after drilling and the gas-hydrate bearing sediments may have been altered more significantly than during the LWD which immediately follows the bit penetration. An important factor in using log data to generate the FF-porosity crossplot is the effect of hydrate in the hole. Measurements for depths well below the BSR may represent the best representation of a no-hydrate/no-gas reference.

It should be noted that estimates of the Archie coefficients may differ for near surface sediments and deeper sediment sections (Novosel, 2002, Riedel et al., 2004). Typically the upper 10 – 20 mbsf show considerably higher porosities than predicted by an upward extrapolation of a deeper trend (e.g. by Athy's law) and result in a much smaller value for the parameter m (Riedel et al., 2004).

Saturation exponent n

The parameter *n* (also called saturation exponent) can be estimated by averaging values for different lithologies (Pearson et al., 1983). A value of 1.94 was for example calculated as a pooled estimate for Site 889 (Collett, 2000). However, modeling showed that the parameter *n* is not constant and is dependent on the grain size distribution and gas hydrate concentration itself (Spangenberg, 2001). Thus, there is no "global" value for the parameter n that can be used for the entire sediment column under investigation.

In the simplification of Archie's law, it is assumed that parameter $m = n$ (Hyndman et al., 1999), so that equation (2) becomes:

$$R_s = a \, R_f \, (S_w \theta)^{-m}. \tag{5}$$

For Site 889/890 this simplification gives hydrate concentrations that are slightly higher by up to 4% than using the full Archie equation (2).

Leg 146 resistivity and porosity data

Using discrete core sample measurements, Hyndman et al (1999) determined the parameter a, and m at Site 889/890 to be 1.41 and 1.76, respectively. A very similar result was obtained at the deep basin Site 888 (a=1.39, m=1.76). They further assumed that n = m, which simplifies the Archie function. These values of *a* and *m* are also similar to those found for deep sea sediment cores from elsewhere (e.g., Wang et al., 1976; Pearson et al., 1983).

Compared to the core data analysis, Collett (2000) found substantially different values for the two parameters *a* and *m*, 0.967 and 2.81 respectively, using data from the downhole neutron and core porosities and the electrical resistivity logs at Site 889/890 assuming that the observed pore-water freshening is not related to gas hydrate dissociation but represents the true *in situ* salinity (**Figure 3a**). He used the above mentioned pooled estimate for the saturation exponent (n=1.94). During ODP Leg 146, porosities were determined from (a) discrete samples taken from the recovered cores, (b) Neutron porosity logs and (c) density-logs. It should be noted that due to enlarged hole diameter the neutron porosity log data are significantly degraded, especially in the upper 80 meters below seafloor (mbsf). The values of *m*=2.81 also is unusually high; the value is commonly near the original Archie estimate of 2.0. Therefore, significant uncertainty

remains in this log-derived determination of the Archie parameters as well as for the core data-derived values.

In the FF-porosity cross-plot the log data from ODP Leg 146 (Site 889A, B) appear to be grouped in two clusters (**Figure 3a**). The cluster with the highest formation factors (and lowest porosities) is formed by data from below the BSR only. As noted above, it is speculated that the high electrical resistivities (and seismic velocities) seen in the logs underneath the BSR may be an artifact of the drilling process, when drilling fluid cooled the formation and resulted in artificial formation of gas hydrate around the bore-hole (Hyndman et al., 2001). Although the results for the Archie parameters by Collett (2000) are very similar to results from Leg 204 (with both locations having very similar tectonic history) it is important to note that the cross-plot results from leg 204 are mainly determined from slope sediments. Drilling and logging during Leg 204 only partially penetrated into accreted sediments, in contrast to Site 889, where large gas hydrate concentrations were estimated for the accreted mélange sediments (below 128 mbsf) and lower concentrations within the upper slope basin sediments.

Results from the reference Site 888 show a significant discrepancy between log-derived and core-derived formation factors (**Figure 3b**). The Archie-parameter estimates by Hyndman et al. (1999) based on the core data were a=1.39, and m=1.76). However, the log data show considerable scatter and hardly any trend.

Leg 204 resistivity and porosity data

During ODP Leg 204 at southern Hydrate Ridge several logs of electrical resistivity were acquired (Trehu et al., 2003). As an example a crossplot of porosity and formation factor derived from LWD ring-resistivity data and neutron-porosity logs at Site 1251 are shown in **Figure 3c**. There is a very good correlation, following Archie's law with empirical coefficients *a* and *m* as 0.967 and 2.81, respectively. However, the core-derived porosity data give a greater scatter with some lower resistivity values. Unfortunately, only low quality core resistivities are available from Site 1251 due to problems in the calibration of the non-contact resistivity tool (Riedel et al., 2004). Thus the discrepancy between the core and the 1251 resistivity LWD data may be a result of

different lithologies. Gas hydrate concentrations calculated from the LWD resistivity data at this Site did not exceed a few percent (Trehu et al., 2003).

Controls of Lithology on Archie's Parameters?

There is an obvious discrepancy between estimates based on core or log-data, and also for which lithology the estimates are determined. In Figure 4 we have plotted all core-derived resistivity data from Leg 204 and Leg 146, color-coded to represent either slope-basin or accreted sediments. While data from Leg 204 show a clear separation between accreted and slope-basin sediments with distinctly different trends, data from Leg 146 (Sites 888 and 889/890) apparently follow exclusively the trend determined by Hyndman et al (1999). Leg 204 data for slope-basin sediments almost follow the trend defined by Collett (2000). A best fit to the Leg 204 slope-basin sediment data is achieved with the Archie parameters a and m as 1.06 and 2.71, respectively. Most of the slope-basin sediments of Leg 146 fall into the range of the Leg 204 data. However, for porosities lower than 0.55, the equivalent formation factors are significantly reduced compared to Leg 204.

The accreted sediments of Leg 204 apparently yield the Archie parameters a=1.68 and m=1.65, which is very close to the parameters determined by Hyndman et al. (1999). Using data for accreted sediment samples from Leg 146 yield the similar range as the Leg 204 data, but also do the slope-basin sediments below a porosity of 0.55.

Data from Leg 204 were determined using a non-contact-resistivity (NCR) tool (Riedel et al., 2005), which measures resistivity of the whole-round core over a total length of 10 cm. During Leg 146 the ODP standard 4-pin Wenner-electrode system was used, which takes measurements on the split core and averages resistivity over a much smaller area. We have no direct comparison of the two tools on the same sediment samples, but will attempt to collect new data with both systems during the IODP Expedition 311.

It should be noted that cores taken in the slope-basin are retrieved with the Advanced-Piston-Coring (APC) system, while accreted sediments are regularly taken with the Extended-Core-Barrel (XCB) system. The XCB cores show signs of infiltration of a mix of mud and seawater into the often broken-up accreted sediments filling cracks

and voids. Thus measurements with the NCR tool or 4-pin Wenner probe on these sediments may result in altered resistivity values. In case where the *in situ* pore-water of accreted sediments may be significantly fresher than seawater, the XCB coring technique would artificially reduce resistivity and thus formation factor by infiltrating a lower-resistive (more saline) pore-water.

A significant challenge is to explain the trend of the Site 888 core resistivity data, where a switch from APC to XCB coring occurred at 330 mbsf. No significant change in the trend of the resistivity-versus-porosity data can be identified, with the data generally following the accreted sediment trend from Sites 889/890 and Leg 204.

Hydrate concentrations

Figure 5 shows the gas hydrate concentrations determined directly from the standard Archie relation (equation 2) for the two different sets of Archie parameters (*a*, *m*, and *n*) and assumptions of *in situ* pore-water resistivity, as well as from the equation by Hyndman et al. (1999), which makes no assumptions about the *in situ* pore-water resistivity.

We also have refined the equation by Hyndman et al. (1999) by a more exact formulation, i.e. introduced the more exact seawater-salinity to resistivity relation by using the equation of state of seawater (Fofonof 1985) and used the full Archie law including a saturation coefficient n=1.94 and recalculated the gas hydrate concentrations with the same empirical values a=1.4 and m=1.76. The result of these changes is a slight reduction in gas hydrate concentration, which becomes more pronounced with depth, but only rarely exceeds a change in hydrate concentration of 5% of the pore volume. The refined estimate gives hydrate concentrations slightly closer to the estimates from the velocity data by Yuan et al., (1996).

Calculations for gas hydrate concentration using the Archie relation of equation (2) based on the assumption that the *in situ* pore-fluid is at a seawater reference does not yield meaningful results for both sets of Archie parameters. Water saturations are in both cases even smaller than -1. If we assume that the pore-water has fresher *in situ* salinity and higher resistivities following the earlier approach describe in the chlorinity section, a more meaningful set of gas hydrate concentrations can be achieved. Using the Archie

parameters by Hyndman et al (1999) yield the highest concentrations, which are on average 30% of the pore space in an interval of 100 m above the BSR. Equivalently, using the Collett (2000) set of parameters yield much smaller concentrations that are on average only 5% of the pore space.

If the original equation by Hyndman et al (1999) is used, no assumptions need to be made about the *in situ* pore-water resistivity. Using the Archie parameters a=1.41, m=1.76 and n=m, gas hydrate concentrations are almost identical to the approach with using Archie's law and a downhole freshening of the pore water. The calculated *in situ* pore-water salinities in this scenario are superimposed on Figure 2b and are slightly lower than the values from Site 888. If the Archie parameters by Collett (2000) are used (a=0.967, m=2.81, n=1.94), the gas hydrate concentration is around zero and the calculated *in situ* pore-water salinities fall exactly on top of the strongly decreasing reference profile.

Two fundamentally different results are obtained based on what the used Archie parameters are and what baseline of pore-water resistivity is assumed. Using the parameters by Collett (2000) favors gas hydrate concentrations that are on average 5% of the pore space and is consistent with low *in situ* pore-water salinities. Parameters determined by Hyndman et al. (1999) yield concentrations that are on average 30% of the pore space and result in slightly lower than seawater pore-water salinities (or the 888 reference).

At this stage no conclusion can be made to whether which of the sets of Archie's Law parameters are correct. Additional research is required to find the cause of the apparent mismatch between core- and log-derived porosity/formation-factors, as well as the potential influence of drilling strategy or lithology on those parameters.

SONIC LOGS AND BACKGROUND VELOCITY PROFILES

Seismic velocity data provide the third method for estimating gas hydrate concentrations. Two fairly high-quality sonic logs were obtained at Site 889. Seismic and sonic P- and S-wave velocities are very sensitive to the presence of gas hydrate. To a

first order, gas hydrate is taken to replace pore-fluid and threfore increase P- and S-wave velocities. S-wave velocities may be altered more strongly if gas hydrate forms in such a way that the overall matrix is stiffened, i.e. hydrate acts as grain cement. However, there usually are limited S-wave data. As for the chlorinity/porosity and resistivity approaches to hydrate concentrations, the reference velocities for no-hydrate and no-gas are the critical parameters.

Velocity versus hydrate concentration

There are several different approaches to define this relation, which can be sorted into three different groups: (a) the time averaging approach (e.g. Yuan et al., 1996; Wood et al., 1941), and using weighted time averaging equations (Lee et al., 1993), (b) rock-physics modeling (e.g. effective medium theory by Helgerud et al., 1999; cementation model by Dvorkin and Nur, 1993, Biot-stoll model by Carcione and Tinivella, 2000), and (c) using empirical porosity-velocity functions and the effective porosity reduction model (e.g. Jarrad et al., 1995; Hyndman et al., 1993; Yuan et al., 1996). A general comparison of the different theoretical methods in (a) and (b) including application to field data has been given recently by Chand et al. (2004). Here we do not repeat their exhaustive analyses but focus on methods using the empirical porosity-velocity functions and the porosity-reduction approach. For comparison purposes we include results using the Lee et al. (1993) weighted time-average equation, which is one of the less computationally intensive equations.

Reference no-hydrate, no-gas velocity-depth profile

In all the empirical methods for obtaining hydrate concentrations from velocity data a critical element is a no-gas, no-hydrate reference velocity depth profile. Such a reference can either be theoretically calculated, determined from regional seismic velocity studies where it is concluded that there is no hydrate or gas (e.g. Yuan et al., 1996), or it can be determined by using downhole porosity logs and empirically derived functions that relate porosity and seismic velocity.

A background velocity profile is then converted to a background porosity profile with the empirical functions. The porosity reduction model assumes that gas hydrate that

formed in the sediments simply replaced the pore-fluid and reduces porosity. Thus, higher than reference seismic velocities give lower than reference porosities and a simple subtraction of the two porosities yield the gas hydrate concentration.

Data examples from ODP Site 889/890

In the following section we use data from two downhole sonic logs from the ODP Site 889 and regional seismic interval velocities around this ODP Site from Yuan et al. (1996). The downhole log data show a steady velocity increase to about 1800 m/s just above the BSR. Below the BSR, one log showed a substantial decrease in velocity to about 1700 m/s and other a smaller decrease. This decrease could be either from the effect of underlying free gas (as shown in the VSP data) or the effect of hydrate generated in from the free gas in an annulus around the borehole by the cool drilling fluid (as discussed above for the resistivity log data). Two simple models were previously used to relate the gas hydrate concentrations to seismic velocities and both methods are based on the assumption that gas hydrate replaces pore fluid in the pore spaces without significantly changing the pore structure (Yuan et al., 1996). One method is to assume that the elevated sonic and interval velocities can be approximated by the simple porosity reduction as outlined above. Another method is based on a time-averaging approach by first combining a velocity of pure hydrate and sediment matrix (no pore-fluid), and then combine that composite matrix with water-saturated sediment to determine an overall velocity (Yuan et al., 1996). Both methods yield approximately the same gas hydrate concentrations that varied between 20% and 30% of the pore volume.

A critical element in the calculations by Yuan et al. (1996) was the background seismic velocity and porosity for no gas and no gas hydrate. A deep velocity profile was determined from seismic interval velocities in an area of 10km around the ODP Site 889/890. Yuan et al. (1996) distinguished two reference profiles: one for the upper slope basin sediments (up to a depth of 130 mbsf at Site 889/890) and one for accreted sediments (deeper than 130 mbsf) based on interval velocity calculations (Yuan et al., 1994). The slope basin velocities are significantly higher than those of the accreted sediments. In a later review Hyndman et al. (2001) simplified the reference profile using

the trend defined from the accreted sediments only and upward extrapolation into the slope-sediment interval.

Porosity-depth from core porosity data

First we fit a smooth profile through the core-porosity data (**Figure 6a**) using Athy's law (Athy, 1930):

$$\Phi = \Phi_0 \, e^{-Z/L,} \tag{4}$$

with Z as depth (mbsf), Φ_0 is the assumed porosity at the seafloor, and L is a characteristic decay constant (here L = 1000 and Φ_0 = 61.5%). In the same graph the neutron porosity log is shown, as well as the porosity reference profile by Yuan et al (1996) as determined from the regional interval velocities and the Hyndman et al (1993) empirical porosity-velocity relation. There is no clear change in trend with depth at the boundary between slope basin and accreted sediments, in either the core or neutron log porosities, in contrast to the velocity data. As noted by Yuan et al., the core and neutron porosity values are significantly lower than those estimated from the interval velocity data (or equivalent higher seismic velocities). The core and neutron porosity profiles are similar to the slope basin profile of Yuan et al. (1996). The break in the Yuan et al. (1996) interval velocity-based reference porosity profile represents the stratigraphic boundary between the slope sediments and accreted sediments at ~130 mbsf. Yuan et al. gave less weight to the neutron porosity estimates because of their low quality.

We calculated background no-hydrate, no-gas porosity-depth profiles based on the smoothed ODP porosity measurements using (a) the Lee et al. (1993) weighted equation, (b) the Hyndman et al. (1993) porosity-velocity relation, and (c) an empirical porosity-velocity relation by Jarrad et al. (1995). Using the Lee et al. (1993) weighted equation yields a seismic velocity of ~1750 m/s at the depth of the BSR (porosity of ~50%). However, this reference profile produces rather large velocities at shallow depth up to 80 mbsf (**Figure 6b**), that are inconsistent with core data and interval velocities. This approach also gives velocities much higher than the interval velocities at depths greater than about 250 m. Using the porosity-velocity relation proposed by Hyndman et al. (1993) a slightly different background velocity can be calculated from the same smooth porosity profile. This background velocity also displays relatively large velocities

at shallow depth but with increasing depth the difference between the Lee et al. (1993) and the Hyndman et al. (1993) equation becomes more significant.

Using the Jarrad et al. (1995) empirical relation, which is based on the ODP Leg 146 data but omitting results from fractured sediment samples, we calculated a third velocity profile for the smooth porosities. This profile is almost parallel to the profile calculated with the Lee et al. (1993) equation, but has lower velocities and appears to be a reasonable overall background profile based on the available data, although it ignores the contrast between slope basin and accreted sediments at about 130 m depth. Similarly, the Lee et al. (1993) weighted equation used constant parameters (especially the weighting factor), which may result in an overestimation of the velocities in the upper 130 mbsf. Increasing the weight-factor yields a decrease in the velocities for the same porosity.

Using the reference profiles defined from the Lee et al. (1993) weighted equation, the empirical relation by Jarrad et al. (1995) and the Hyndman et al. (1993) relation we calculated gas hydrate concentrations for the 889/890 sonic logs assuming the simple porosity reduction model. As seen in **Figure 6c**, the Lee weighted equation yields the smallest gas hydrate concentrations with a maximum of 15% of the pore space, but on average the concentrations are below 5%. Results using the Hyndman et al (1993) relation (**Figure 6d**) are relatively similar to those using the Jarrad et al. (1995) relation (**Figure 6e**) for depth below 200 mbsf. However, at shallower depth, they differ more significantly. The result from the Jarrad et al. (1995) reference yields the highest concentrations; however they are still significantly below 20% on average. Using the Yuan et al. (1996) velocity (and porosity) reference profile results in the largest gas hydrate concentration (**Figure 6f**). They are on average 20% over the interval in the accreted sediments, but occasionally exceed up to 30% (Yuan et al., 1996; Hyndman et al., 2001).

Leg 204 Hydrate Ridge velocity-depths as a reference

In comparison with the Site 889/890 data, low sonic P-wave velocities were obtained at Leg 204 Sites 1244 and 1245 (**Figure 7**). The BSR at these Sites is relatively shallow at 127 mbsf, and 134 mbsf, respectively. The entire logged sequences at all Sites consist of slope sediments similar to those with in the upper 130 mbsf at Site 889 of ODP Leg 146. The two regions have similar velocities for the upper 100 m, but at greater

depth the Hydrate Ridge velocities are much lower. At a depth of 200 mbsf at all these Sites the P-wave sonic velocity is only at around 1580 m/s, whereas at Site 889, a velocity of almost 1800 m/s was measured (though still within hydrate-bearing sediments). However, the sonic-logs at Sites 1244 and 1245 are in very good agreement with results from regional MCS and Ocean Bottom Hydrophone velocity analyses (Papenberg, 2004). A composite analysis of all gas hydrate proxies at the Sites 1244 and 1245 yielded average gas hydrate concentrations of less than 5% and thus no strong velocity changes were observed. If the Hydrate Ridge velocity-depth profiles are used as a no-hydrate reference, the hydrate concentration estimates from Site 889/890 velocity logs are even greater than those using the Yuan et al. (1996) reference.

Summary and Conclusion

A re-evaluation of hydrate concentrations was suggested after results from ODP Leg 204 at southern Hydrate Ridge showed very small gas hydrate concentrations on average (except for the unusual summit vent Sites 1249, 1250) in a tectonically very similar setting than the ODP Leg 146, Site 889/890 location (Trehu et al., 2004). We have re-evaluated calculations of gas hydrate concentrations at the Northern Cascadia Margin using ODP Leg 146 sonic and electrical resistivity logs and pore-water chlorinity/salinity data. Earlier analyses showed gas hydrate concentrations that varied on average between 20 and 35% of the pore volume (see summary by Hyndman et al., 2001 and references therein). Our re-visiting of the methods used show that there are large uncertainties in the concentrations. They could be as low as 5-10% and as high as 30% average of the pore volume from about 130 mbsf to the BSR (at ~230 mbsf) if different in situ pore fluid resistivities (salinity), and different no-hydrate reference velocity-depth profiles are used in the calculations.

No conclusive estimate can be made using the chlorinity (salinity) baseline without additional pore-water chemistry data (lithium and strontium data) to confirm that the model by Torres et al. (2004) is also valid for the Site 889/890 of ODP Leg 146. Therefore the gas hydrate concentration based on chlorinity data may either be as low as a few percent (as also suggested earlier by Ussller and Paull, 2001) or as high as 40% previously suggested by Hyndman et al. (1999).

Gas hydrate concentrations were also calculated from the resistivity data using Archie's-law. Archie's law consists of several empirical parameters (referred to as a, m, and n), which were determined to a=1.4, m=1.76, and n=1.0 by Hyndman et al., (1999) using the ODP Leg 146 core data at Site 888 and 889/890. However, Collett (2000) also estimated these parameters to a=1.0, m=2.8, n=1.9 by using the ODP Site 889 resistivity and neutron porosity logs. The differences in these empirical parameters result in substantially different gas hydrate concentrations. The ODP log data are of relatively poor quality and neither our new parameters nor the previous analyses fit all data well and a large uncertainty remains in the results. However, LWD log results from ODP Leg 204, obtained from a tectonically similar environment, suggest the Archie parameters by Collett (2000) may be preferable.

Finally a number of approaches to no-hydrate velocity references were calculated for Site 889, including porosities using various published empirical relations between porosity and velocity (Jarrad et al., 1995; Hyndman et al., 1993) and the Lee et al. (1993) weighted equation. Some of these baselines have significantly higher seismic velocities compared to that of Yuan et al. (1996). Thus they result in gas hydrate concentrations that are only between 5 and 10% on average of the pore volume only. Substantial uncertainty remains in the applicability of the empirical parameters for each of the individual equations. If the LWD log velocity-depth data from Leg 204 is used as a no-hydrate reference, the computed hydrate concentrations at Site 889/890 are even higher than those of Yuan et al. (1996).

References

Athy, L. F., 1930. Density, porosity, and compaction of sedimentary rocks. *AAPG Bull.,* 14:1-24.

Blum, P., 1997. Physical properties handbook: a guide to the shipboard measurement of physical properties of deep-sea cores. *ODP Tech. Note*, 26.

Carcione, J. M., and U. Tinivella, 2000. Bottom-simulating reflectors: Seismic velocities and AVO effects, Geophysics, 65, 54–67.

Chand, S., T.A. Minshull, D. Gei, and J.M. Carcione, 2004. Elastic velocity models for gas-hydrate-bearing sediments – a comparison, Geophys. J. Int., 159, 573 – 590.

Chapman, R., J. Gettrust, R. Walia, D. Hannay, G.D. Spence, W. Wood, and R.D. Hyndman, High resolution deep-towed multichannel seismic survey of deep sea gas hydrates off western Canada. Geophysics, Vol. 67, 1038-1047, 2002.

Collett, T.S., 2000. Quantitative well-log analysis of in-situ natural gas hydrates, PhD thesis, University Colorado school of Mines.

Collett, T.S., 2001. A review of well-log analysis techniques used to assess gas-hydrate-bearing reservoirs, in: Natural gas Hydrates, Occurrence, Distribution and Detection, (ed. C.K. Paull and W.P. Dillon), Geophysical Monograph Series No. 124, pp. 189 – 210, American Geophysical Union (AGU).

Collett, T. S., and J. Ladd, 2000. Detection of gas hydrate with downhole logs and assessment of gas hydrate concentrations (saturations) and gas volumes on the Blake Ridge with electrical resistivity log data, *in* Paull, C.K., Matsumoto, R., Wallace, P.J., and Dillon, W.P., eds., Proceedings of the Ocean Drilling Program, Scientific Results, vol. 164, p. 179 – 191.

Dvorkin, J. and A. Nur. Rock physics for characterization of gas hydrates, in: The future of energy gases. U.S. Geological Survey Professional paper 1570, 1993.

Edwards, R.N., 1997. On the resource evaluation of marine gas hydrate deposits using a seafloor transient electric dipole-dipole method, Geophysics, 62, 63-74.

Fink, C.R. and Spence, G.D. 1999. Hydrate distribution off Vancouver Island from multi-frequency single channel seismic reflection data, J. Geophys. Res., 104, 2909-2922.

Fofonoff, 1985. Physical properties of seawater. J. Geophys. Res., Vol 90 No. C2, pp 3332-3342.

Ganguly, N., G.D. Spence, N.R. Chapman and R.D. Hyndman. 2000. Heat flow variations from bottom simulating reflectors on the Cascadia margin. Marine Geology, 164, 53-68.

Gettrust, G., W. Wood, D. Lindwall, R. Chapman, R. Walia, D. Hannay, G.Spence, K. Louden, R. MacDonald, and R.D. Hyndman. 1999. New seismic study of deep sea gas hydrates results in greatly improved resolution. EOS, 80, 439-440.

Hesse, R., 2003. Pore water anomalies of submarine gas hydrate zones as a tool to assess hydrate abundance and distribution in the subsurface. What have we learned in the past decade? Earth Sci. Rev. 61, 149-179.

Hesse, R., and W.E. Harrison, Gas hydrates (clathrates) causing pore-water freshening and oxygen-isotope fractionation in deep-water sedimentary sections of terrigenous continental margins, Earth Planet. Sci. Lett., 55, 453-462.

Helgerud, M.B., J. Dvorkin, A. Nur, A. Sakai, and T.S. Collett, 1999. Elastic-wave velocity in marine sediments with gas hydrate: effective medium modelling, Geophys. Res. Lett., 26, 2021 – 2024.

Hobro, J.W., 1999. Three-dimensional tomographic inversion of combined reflection and refraction travel-time data, Ph.D. thesis, University of Cambridge, U.K.

Hyndman, R.D., G.D. Spence, R. Chapman, M. Riedel, and R.N. Edwards, Geophysical studies of marine gas hydrate in northern Cascadia. Natural Gas Hydrates: Occurrence, Distribution, and Detection, AGU Monograph, Vol. 124, 273-295, 2001.

Hyndman, R.D., T. Yuan, and K. Moran, The concentration of deep sea gas hydrates from downhole electrical resistivity logs and laboratory data. Earth Planet. Sci. Lett., Vol. 172, 167-177, 1999.

Hyndman, R.D. and Spence, G.D., 1992. A seismic study of methane hydrate marine bottom simulating reflectors, J. Geophys. Res., 97; 5, 6683-6698.

Hyndman, R.D., G.F. Moore, and K. Moran, 1993. Velocity, porosity, and pore-fluid loss from the Nankai subduction zone accretionary prism, Proc. Ocean Drill. Program, Sci. Results, 131, 211 – 220.

Jarrard, R.D., MacKay, M.E., Westbrook, G.K., and Screaton, E.J., 1995, Log-based porosity of ODP sites on the Cascadia accretionary prism, *in* Carson, B., Wettbrook, G.K., Mustgrave, J.R., Suess, E., eds., Proceedings of the Ocean Drilling Program, Scientific Results 146 (pt. 1), College Station, TX, (Ocean Drilling Program), p. 313-335.

Kastner, M., Kvenvolden, K.A., Whiticar, M.J., Camerlenghi, A., and Lorenson, T.D., 1995. Relation between pore fluid chemistry and gas hydrate associated with bottom-simulating reflectors at the Cascadia Margin, Sites 889 and 892, Proc. of

the ODP, Scientific Resutls, 146 (Part 1), College Station, TX (Ocean Drilling Program), 175 – 187, 1995.

Kvenvolden, K.A., 1998, A primer on the geological occurrence of gas hydrate, *in* Henriet, J.-P. and Mienert, J., eds., Gas Hydrates: Relevance to World Margin Stability and Climatic Change: Geological Society Special Publication No. 137, p. 9-30.

Lee, M.W., Hutchinson, D.R., Dillon, W.P., Miller, J.J., Agena, W.F., and Swift, B.A., 1993. Method of estimating the amount of in-situ gas hydrates in deep marine sediments, Marine and Petroleum Geology, 10, 496 – 506.

MacKay, M.E., R.D. Jarrard, G.K. Westbrook, R.D. Hyndman, and the Shipboard Scientific Party of ODP Leg 146, 1994. Origin of bottom simulating reflectors: Geophysical evidence from the Cascadia accretionary prism, Geology, 22, 459-462.

Novosel, I., 2002, Physical properties of gas hydrate related sediments offshore Vancouver Island [M.Sc. Thesis]: University of Victoria, Canada.

Papenberg, C, 2004. Seismic Investigations of a Bottom Simulating Reflector: Implications on Gas Hydrate and Free Gas at Southern Hydrate Ridge, PhD thesis, University of Kiel, Germany.

Paull, C.K., Matsumoto, R., Wallace, P., and et al., Proceedings of the Ocean Drilling Program, Initial Reports 164, Ocean Drilling Program, College Station, TX, 623pp, 1996

Pearson, C.F., Halleck, P.M., McGulre, P.L., Hermes, R., and M. Mathews, 1983. Natural gas hydrate; A review of in situ properties, J. Phys. Chem., 87, 4180 – 4185.

Riedel, M., R.D. Hyndman, G.D. Spence, and R. Chapman, Seismic investigations of an apparent active vent field associated with gas hydrates, offshore Vancouver Island. J. Geophys. Res., Vol. 107, 5-1 to 5-16, 2002.

Riedel, M., P. Long, C.S. Liu, P. Schultheiss, T. Collett, and ODP Leg 204 Shipboard Scientific Party, 2004. Physical properties of near surface sediments at Hydrate Ridge – Results from ODP Leg 204 (in press).

Serra, O., 1984. Fundamentals of well-log interpretation. Developments in Petroleum Science, v.1, Elesevier Publishing, Amsterdam, The Netherlands.

Solem, R.C., Spence, G.D., Vukajlovich, D., Hyndman, R.D., Riedel, M., Novosel, I., and Kastner, M., 2002, Methane advection and gas hydrate formation within an active vent field offshore Vancouver Island: Proceedings of the Fourth International Conference on Gas Hydrates, Yokohama, May 19-23, 2002.

Spangenberg, E., 2001. Modeling of the influence of gas hydrate content on the electrical properties of porous sediments, J. of Geophys. Res., Vol. 106, No. B4, 6535 – 6548, April 2001.

Spence, G.D., T.A. Minshull, and C. Fink, Seismic structure of methane gas hydrate, offshore Vancouver Island, Proc. Ocean Drill. Program, Sci. Results 146, 163-174, 1995.

Spence, G.D., R.D. Hyndman, N.R. Chapman, M. Riedel, N. Edwards, and J. Yuan, 2000. Cascadia margin, northeast Pacific Ocean: Hydrate distribution from geophysical observations. Natural Gas Hydrate in Oceanic and Permafrost Environments, Kluwer Acad. Publ., 183-198.

Timur, A., Velocity of compressional waves in porous media at permafrost temperature, Geophysics, 41, 621{645, 1968.

Tomaru, H., R. Matsumoto, H. Lu, and T. Uchida, Geochemical process of gas hydrate formation in the Nankai Trough based on chloride and isotopic anomalies in interstitial water, Resource Geology, 54, 45-51, 2004.

Torres, M.E., B.M.A. Teichert, A.M. Trehu, W. Borowski, and H. Tomaru, 2004. Relationship of pore water freshening to accretionary processes in the Cascadia margin: fluid sources and gas hydrate abundance, submitted to EPSL.

Trehu, A.M., Bohrmann, G., and Leg 204 Scientific Party, 2003, Proc. of the Ocean Drilling Program, Initial Reports Leg 204, College Station, TX.

Trehu A.M., G. Bohrmann, F.R. Rack, T.S. Collett, D.S. Goldberg, P. E. Long, A.V. Milkov, M. Riedel, P. Schultheiss, M.E. Torres, N.L. Bangs, S.R. Barr, W.S. Borowski, G.E. Claypool, M.E. Delwiche, G.R. Dickens, E. Gracia, G. Guerin, M. Holland, J.E. Johnson, Y-J. Lee, C-S. Liu, X. Su, B. Teichert, H. Tomaru, M. Vanneste, M. Watanabe, J.L. Weinberger., 2004, Three-dimensional distribution of gas hydrate beneath southern Hydrate Ridge: constraints from ODP Leg 204, Earth and Planetary Science Letters, in press).

Ussler III, W., and C.K. Paull, 2001. Ion Exclusion associated with marine gas hydrate deposits, in: Natural Gas Hydrates: Occurrence, Distribution, and Detection, AGU Monograph, Vol. 124, 41 – 65.

Wang, M.C., V.A. Nacci, C.D. Markert, Electrical resistivity method for marine sediment consolidation study, Proc. 8th Annual Offshore Technology Conference, Houston, TX, Paper 2623, 1976.

Westbrook, G., Carson, B., Musgrave, R., 1994, Shipboard Scientific Party, Proc. of the Ocean Drilling Program, Initial Reports Leg 146A, College Station, TX.

Wood, A.B. A textbook of Sound, 578 pp. Macmillan, New York, 1941.

Yuan, T., G.D. Spence, and R.D. Hyndman, 1994. Seismic velocities and inferred porosities in the accretionary wedge sediments at the Cascadia margin, J. Geophys. Res., 99(B3), 4413 – 4427.

Yuan, T., R.D. Hyndman, G.D. SPENCE, and B. Desmons. 1996. Velocity structure of a bottom-simulating reflector and deep sea gas hydrate concentrations on the Cascadia continental slope, Journal of Geophysical Research, 101, 13655-13671

Yuan, T, Hyndman, R.D., Spence, G.D., Minshull, T.A., and Singh, S.C. 1999. Seismic velocity studies of a gas hydrate bottom-simulating reflector on the northern Cascadia continental margin: Amplitude modelling and full waveform inversion, J. Geophys. Res., 104, 1179-1191.

Yuan, J., and Edwards, N., 2001. Towed seafloor electromagnetics and assessment of gas hydrate deposits , Geophys. Res. Lett. 27; 16, 2397-2400.
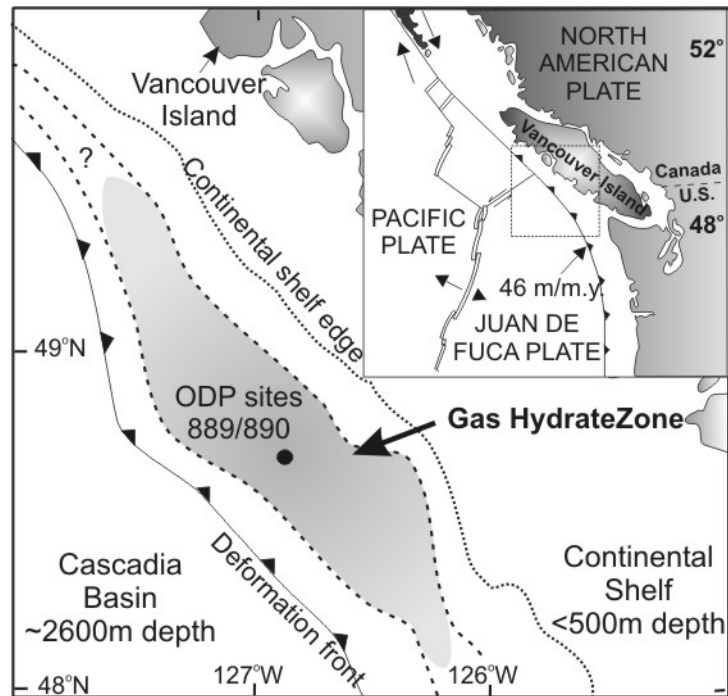
Figure 1

Location of the ODP Site 889/890 on the Northern Cascadia Margin. The gray-shaded area is the assumed zone of gas hydrate occurrence based on the regional distribution of BSRs in seismic data.
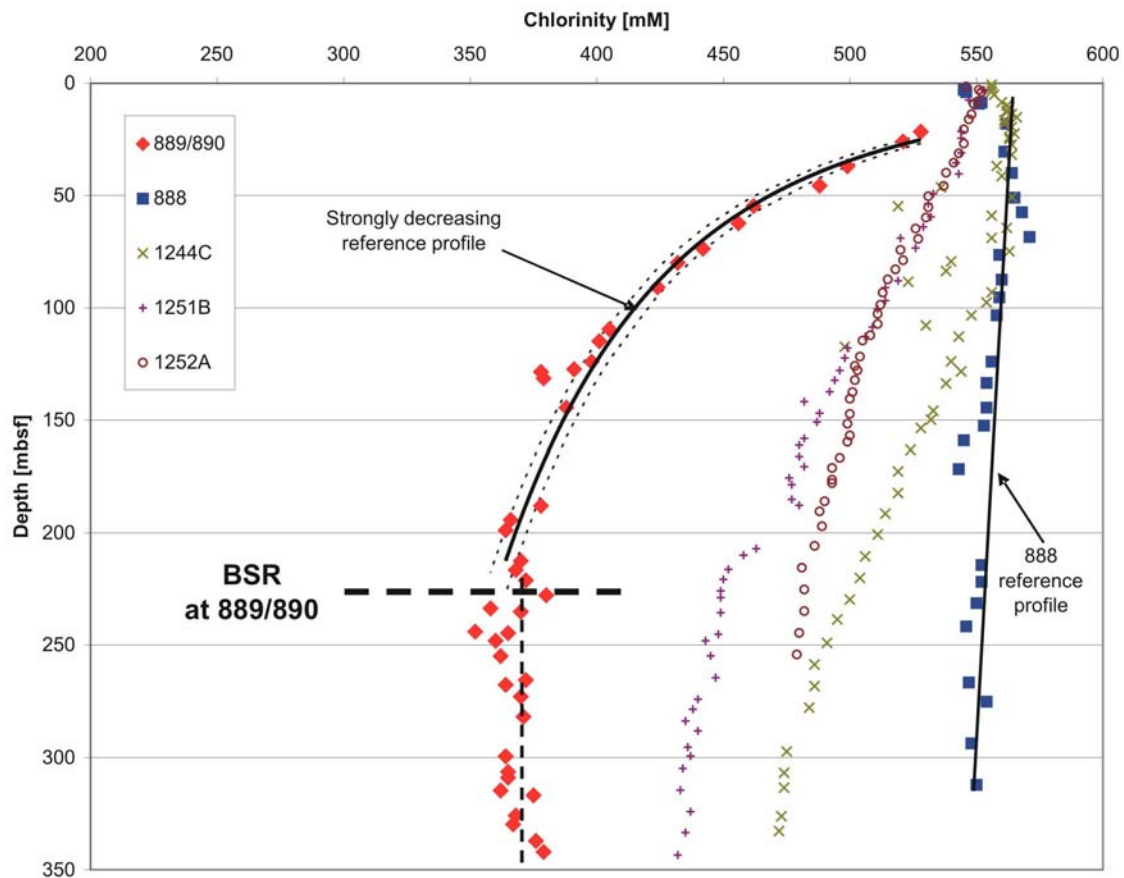
Figure 2a

Chlorinity data from ODP Site 889/890 (red triangles) and decreasing reference profile. A minimum and maximum profile is also indicted by the dashed lines. In comparison chlorinity data from ODP Leg 146, Site 888, and ODP Leg 204, Sites 1244, 1251 and 1252 are shown.
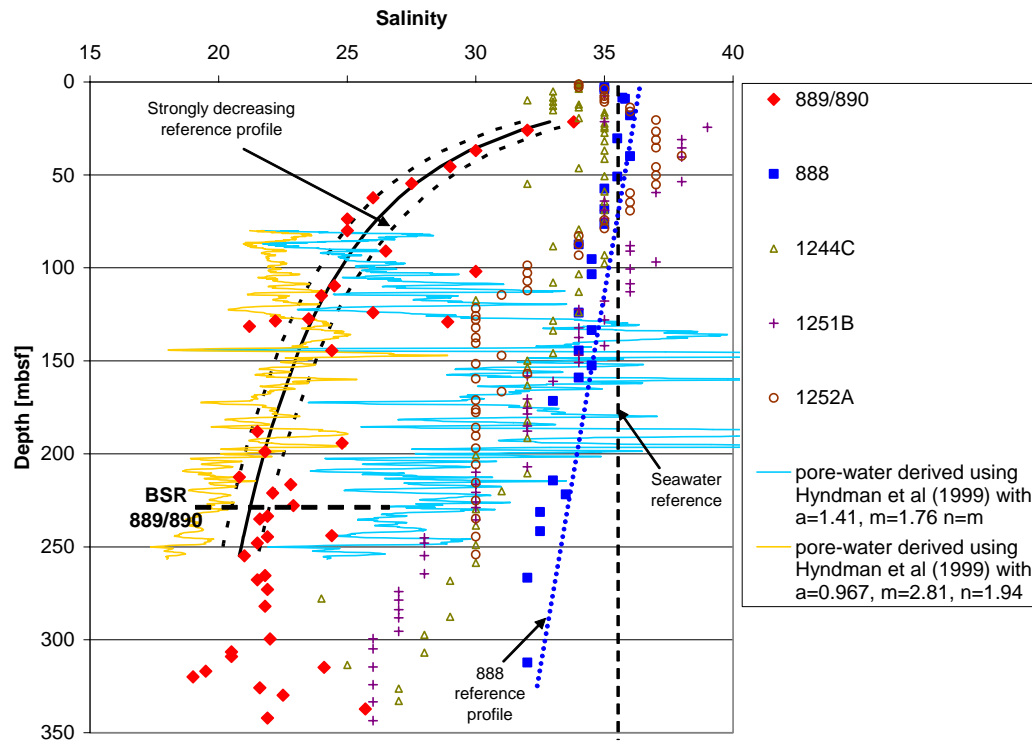
Figure 2b

Pore-water salinity from ODP Leg 146 Site 889/890 with new reference profile. The profile decreases towards the BSR. The two dashed lines represent minimum and maximum possible reference profiles. Data from Sites 888 (Leg 146), and 1244, 1251, and 1252 (Leg 204) were added for comparison. Data from Leg 204 were reported as integer numbers only. Vertical dashed line is seawater reference at 35 PSU.
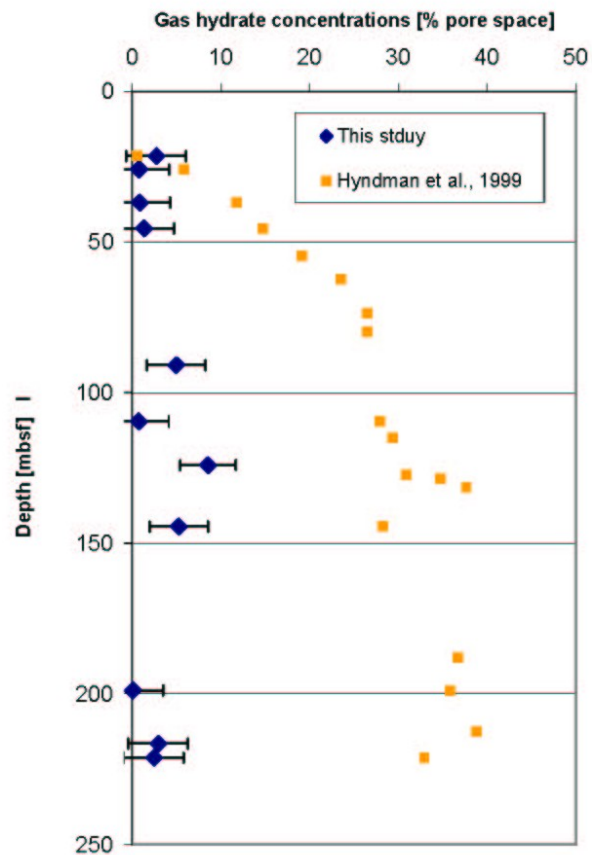
Figure2c

Gas hydrate concentrations calculated from pore-water freshening using the new reference baseline (blue diamonds) and previous concentrations by Hyndman et al., (1999) using a seawater reference (orange squares). Error bars were calculated using the minimum and maximum reference profile from Figure 2b.
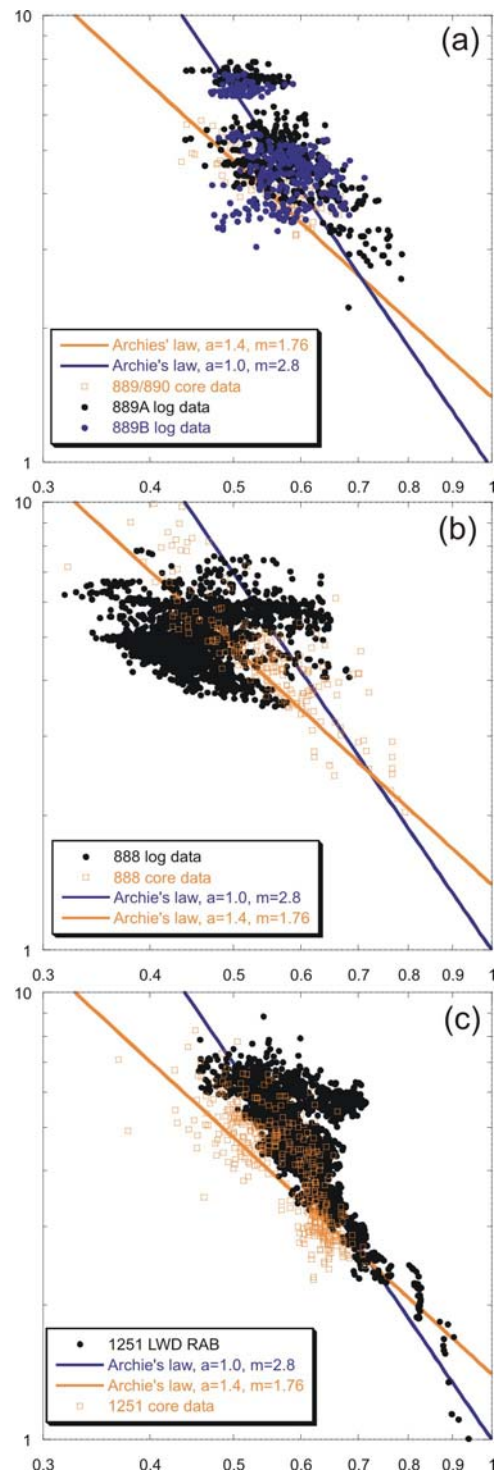
Figure 3. Crossplots of Formation Factor (FF) and porosity for (a) ODP Leg 146, Site 889A/B, (b) ODP Leg 146 Site 888, and (c) ODP Leg 204, Site 1251; Core data are from all Sites at Leg 204.
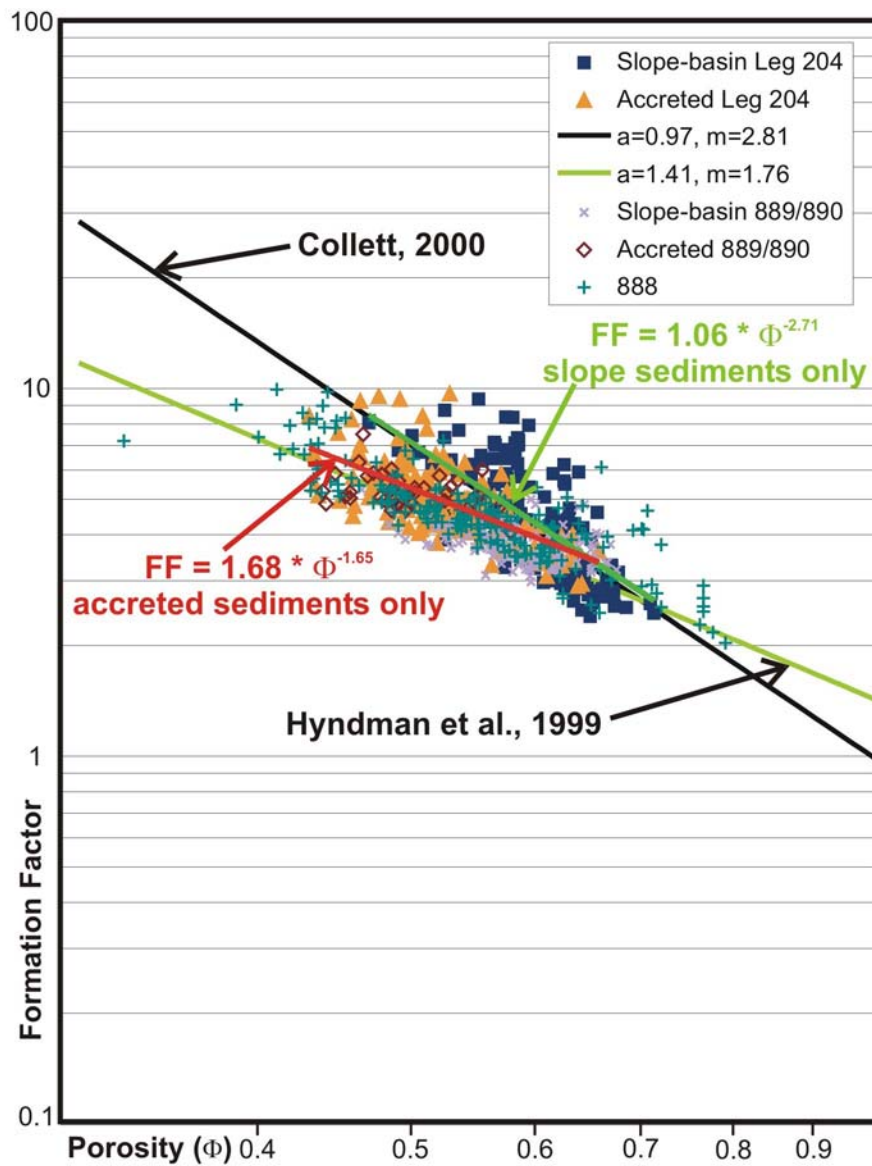
Figure 4: Crossplot of Formation Factor (FF) for core-derived data only from ODP Leg 204 and Leg 146 color-coded for general lithology (slope-basin or accreted sediments).
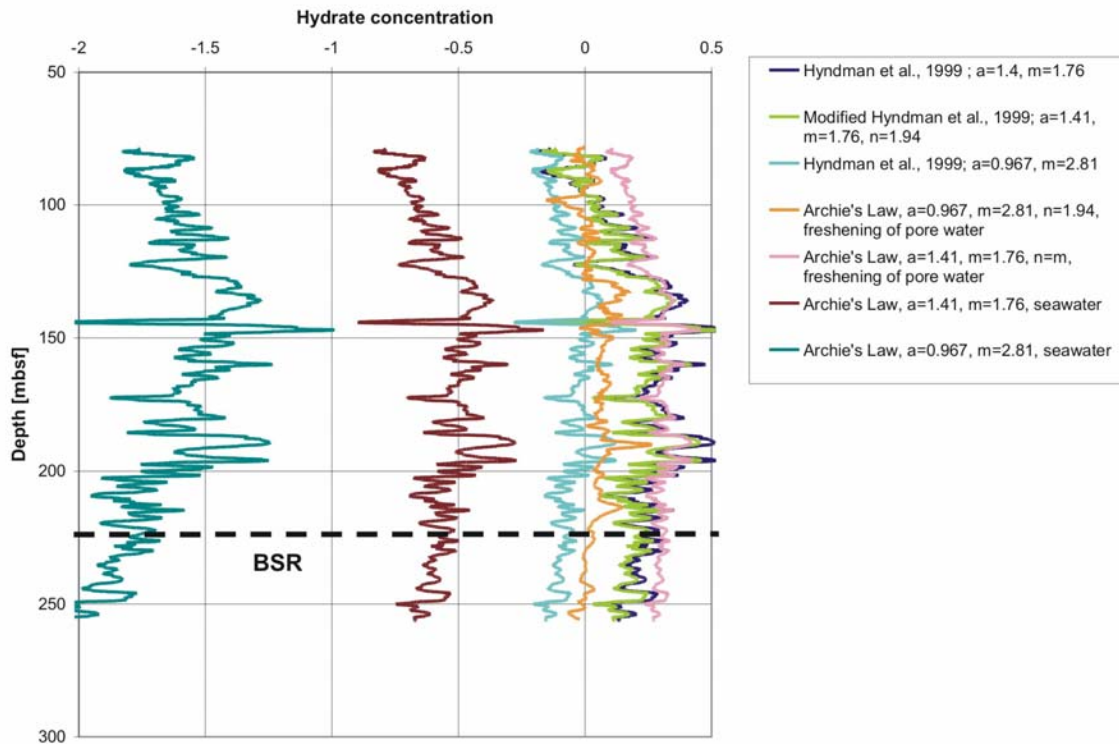
Figure 5:

Standard- Archie-derived gas hydrate saturations (Sh) calculated from the downhole electrical resistivity log at Hole 889B using different sets of Archie's Law parameters (a) a=0.967, m=2.81, n=1.96 (Collett (2000), (b) a=1.41, m=1.76, n=1 (Hyndman et al., 1999) and (c) a=1.41, m=1.76, n=1.96 (modified Hyndman et al. (1999) equation) as well as different assumptions about the *in situ* pore water salinity (at seawater reference or freshening with depth as defined from downhole decrease in Figure 2b).
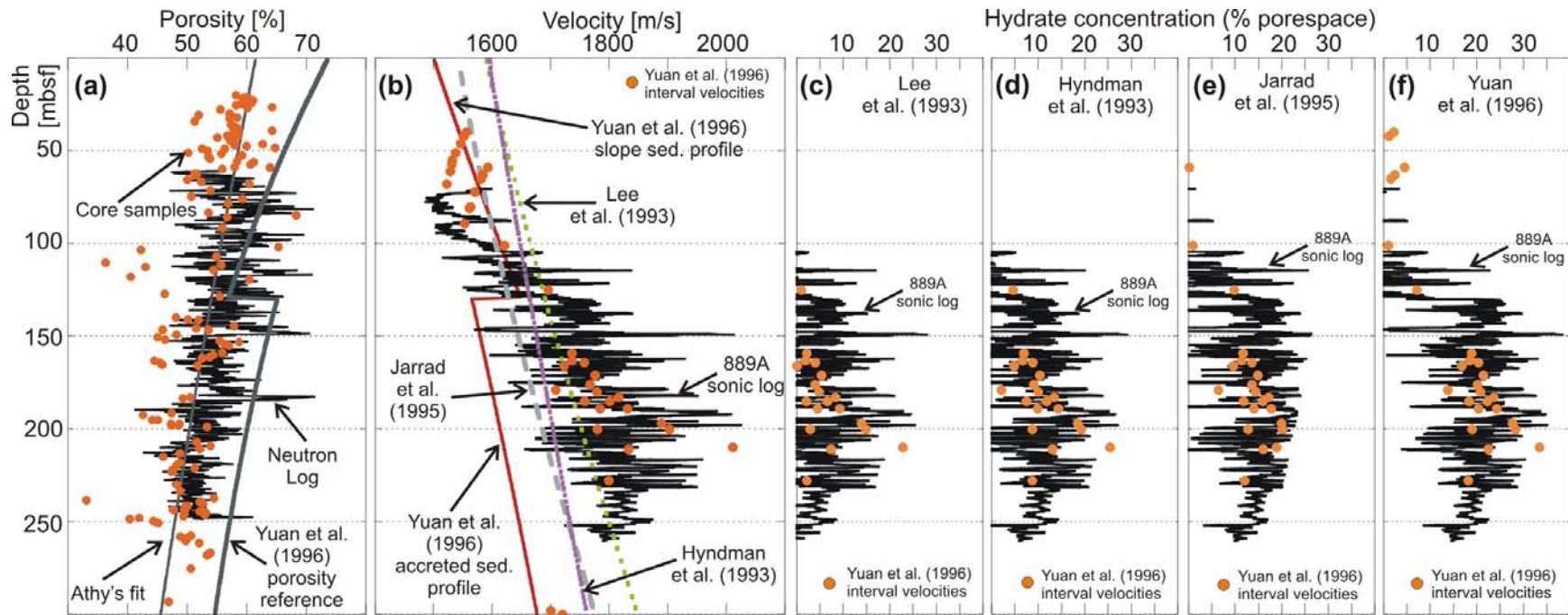
Figure 6.

(a) Core porosities from ODP Site 889/890, smoothed porosity profile after Athy's law (Athy, 1930), neutron porosity log at Site 889, and Yuan et al. (1996) porosity reference porfile; (b) Reference velocity profiles; ODP Site 889/890 sonic log and seismic interval velocities; Gas hydrate concentrations from (c) the Lee et al. (1993) equation reference, (d) the Hyndman et al. (1993) reference with an empirical porosity-velocity function, and (e) the Jarrad et al. (1995) reference with a slightly revised empirical porosity-velocity function.
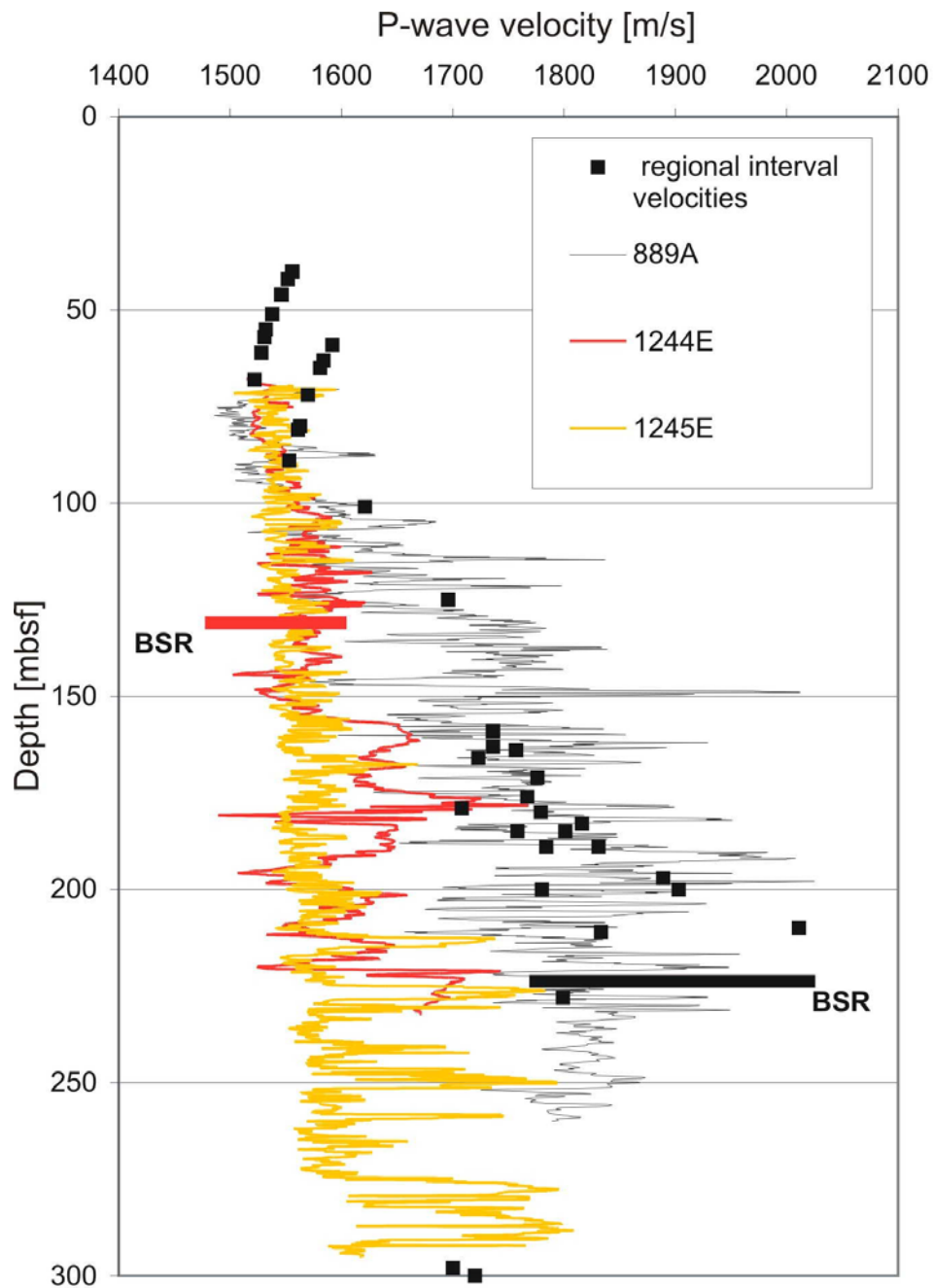
Figure 7. Sonic logs from ODP Leg 146 Site 889 (black), ODP Leg 204 Site 1244 (red) and Site 1245 (yellow). Approximate depth of the BSR are shown at each of the Sites, respectively. Regional interval velocities near Site 889 are also shown (black squares).

Appendix

The Hyndman et al (1999) equation to estimate gas hydrate concentration (S) from electrical resistivity data is given by:

S = 1 – A,

With A given by:

A= (1 / Φ) [(a C_{sw} R_{sw})/(Φ C_{corefl} R_{fm})] $^{(1/m-1)}$,

Where

Φ is porosity, C_{sw} is salinity of seawater reference, R_{sw} is resistivity of seawater reference, R_{fm} is in situ formation resistivity (from log), and C_{corefl} is pore fluid salinity measured in the recovered cores.